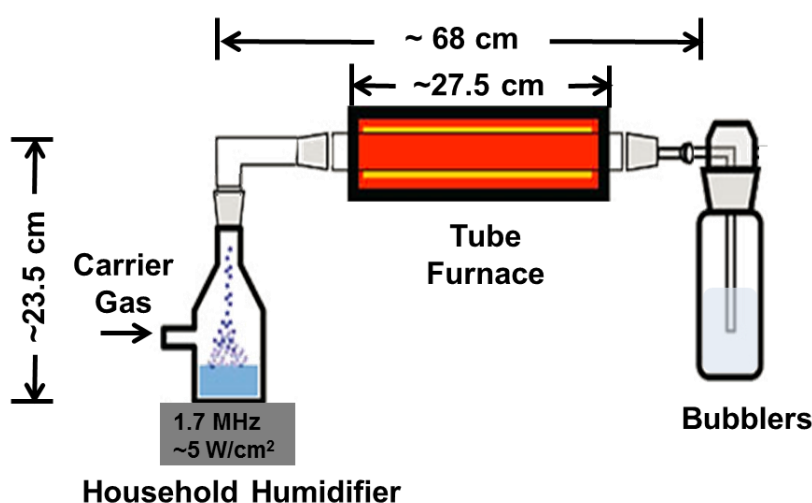


## Supporting Information

### Aerosol Synthesis of Shape-Controlled Template Particles: a Route to Ta<sub>3</sub>N<sub>5</sub> Nanoplates and Octahedra as Photocatalysts

Jie Fu and Sara E. Skrabalak\*

Department of Chemistry, Indiana University, Bloomington, Indiana 47405, United States



**Figure S1.** Schematic of experimental setup for aerosol-assisted molten salt synthesis.

The nebulization source consists of a Vicks V5100N Ultrasonic Humidifier base (1.7 MHz, ~5 W/cm<sup>2</sup>) filled with water as the media. The nebulization chamber has a gas inlet and an opening (diameter ~52 mm) with an O-ring groove (Chemglass: CG-138-02) at the bottom. A Saran wrap membrane is clamped between a Teflon base with a greased O-ring and the nebulization chamber. The nebulization chamber is then centered above the ultrasonic transducer at a distance of ~2 cm and filled with ~15 mL of precursor solution (room temperature). A stainless steel tube (inside diameter ~2.5 cm, length ~52 cm) is used with the single zone furnace (total heating region of ~27.5 cm, 1100 °C maximum).

Note: while a Vicks V5100N Ultrasonic Humidifier base was used in the study, the system is adaptable to other household humidifiers and small changes in dimensions without changing the properties of the product.

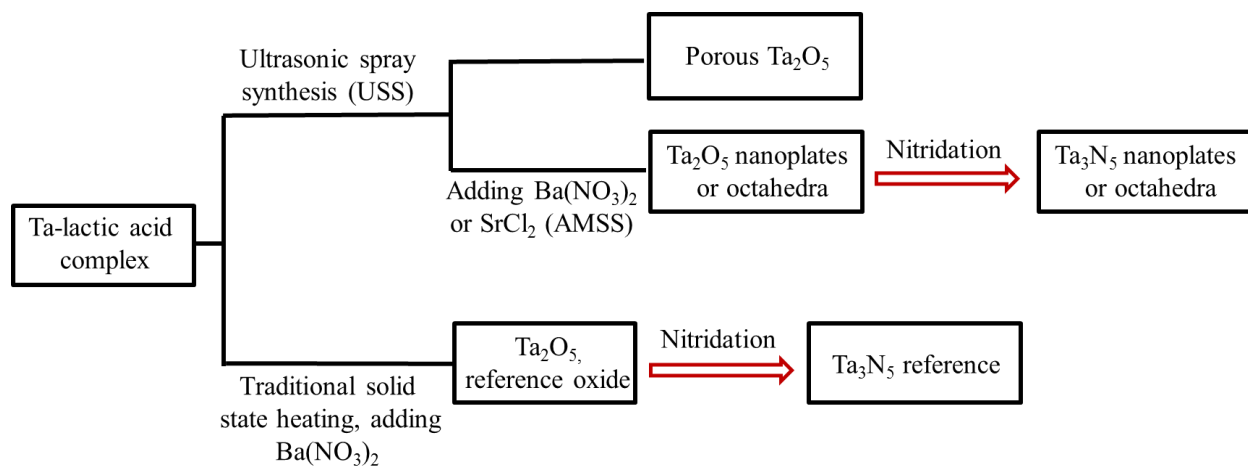


**Figure S2.** A block diagram of the synthetic routes for the main products.

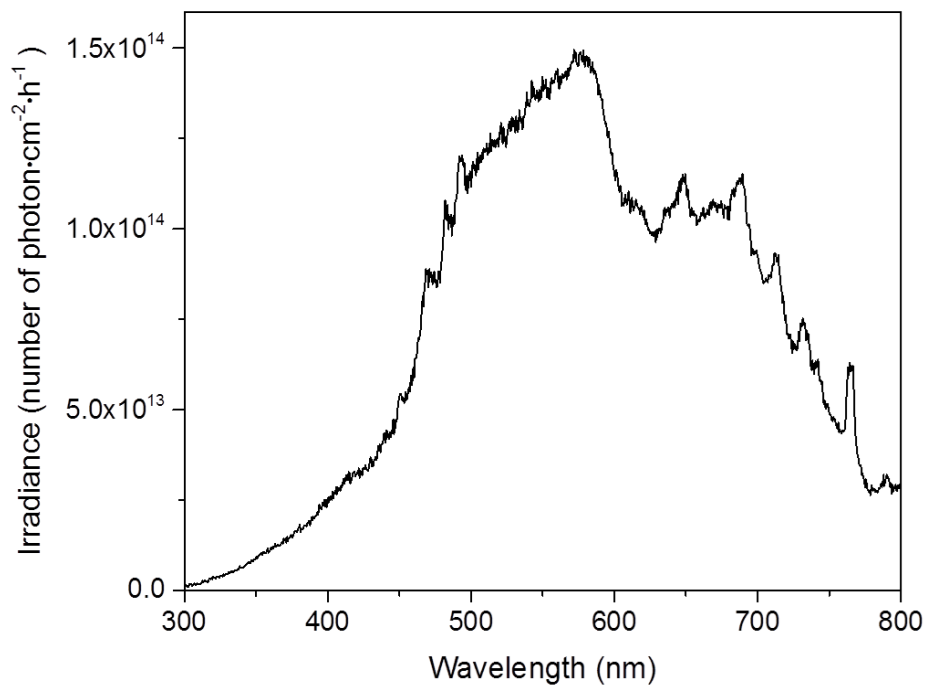


**Figure S3.** Flux irradiance of the xenon light source used for photocatalysis.

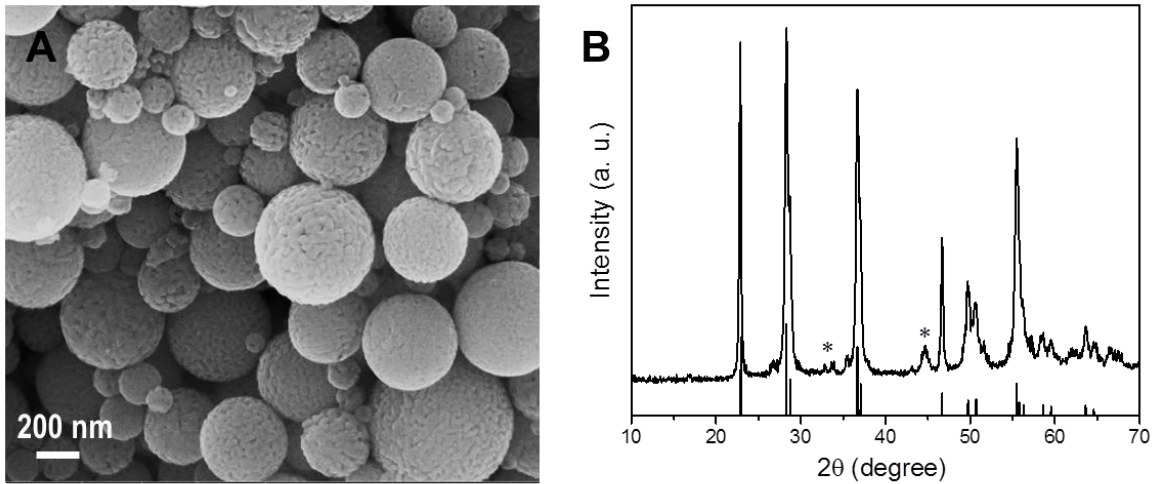


**Figure S4.** (A) SEM image and (B) XRD of  $\text{Ta}_2\text{O}_5$  microspheres prepared by USS. Reference  $\text{Ta}_2\text{O}_5$  ICDD # 01-089-2843, with an impurity denoted with asterisks in the XRD pattern.

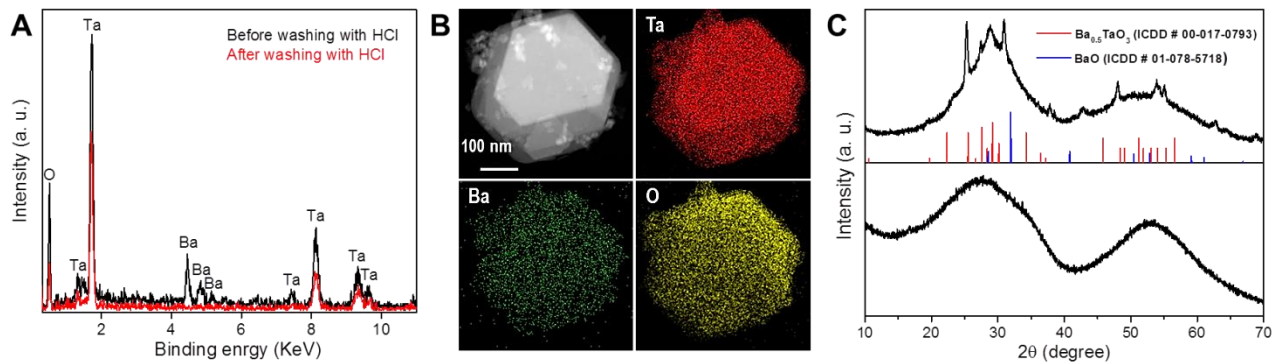


**Figure S5.** (A) EDX analysis of  $\text{Ta}_2\text{O}_5$  nanoplates before and after washing with HCl, (B) STEM image (upper left panel) and elemental mapping by STEM-EDX of an individual nanoplate before washing with HCl (red corresponds to Ta, green corresponds to Ba, and yellow corresponds to O), (C) XRD patterns of  $\text{Ta}_2\text{O}_5$  nanoplates before (top panel) and after (bottom panel) HCl washing.

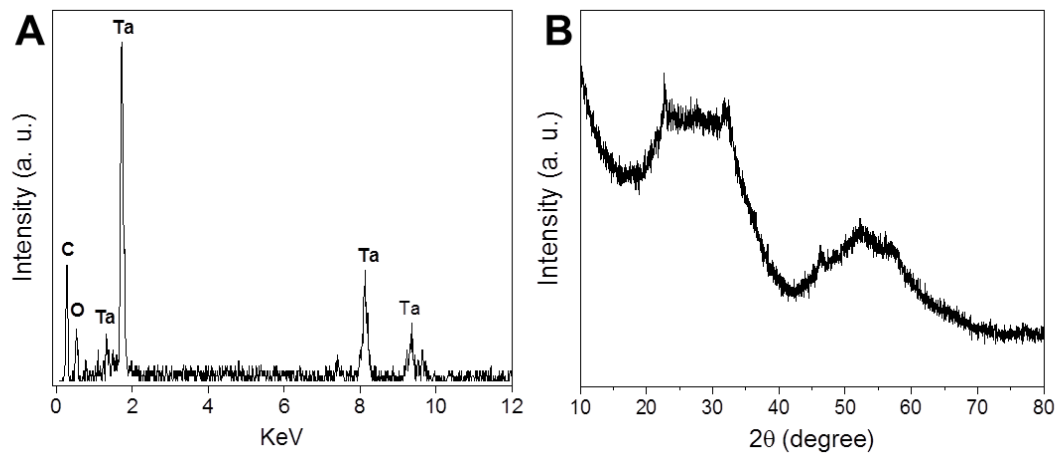


**Figure S6.** (A) EDX analysis and (B) XRD pattern of Ta<sub>2</sub>O<sub>5</sub> octahedra.

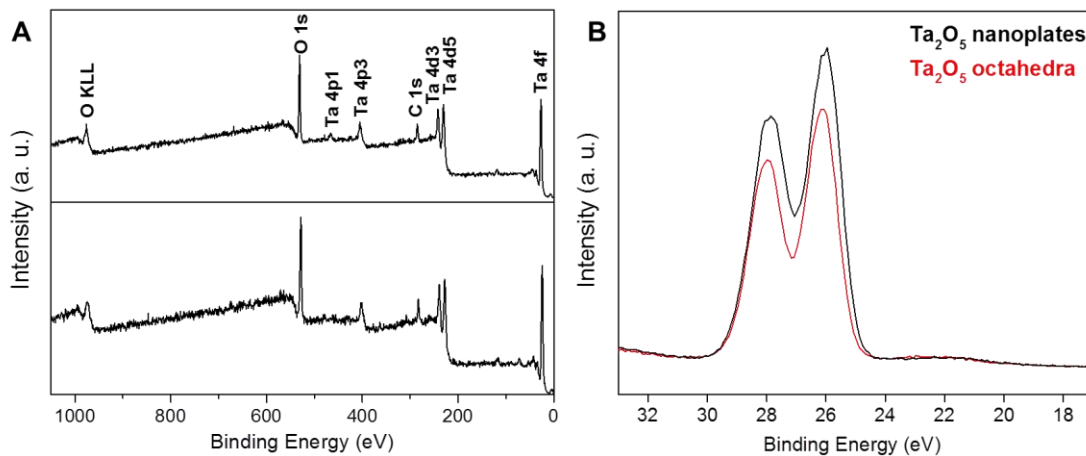


**Figure S7.** (A) The survey XPS spectra of Ta<sub>2</sub>O<sub>5</sub> nanoplates (top panel) and octahedra (bottom panel). (B) High resolution XPS spectra of Ta 4f region for Ta<sub>2</sub>O<sub>5</sub> nanoplates and octahedra.

|   | C    | H    | N     |
|---|------|------|-------|
| Ta <sub>2</sub> O <sub>5</sub> nanoplates | 0.40 | 1.04 | 0     |
| Ta <sub>2</sub> O <sub>5</sub> octahedra  | 0.35 | 0.73 | 0     |
| Ta <sub>3</sub> N <sub>5</sub> nanoplates | 0.02 | 0    | 10.92 |
| Ta <sub>3</sub> N <sub>5</sub> octahedra  | 0.03 | 0    | 10.76 |
| Ta <sub>3</sub> N <sub>5</sub> reference  | 0.03 | 0    | 10.96 |

**Table S1.** A table of CHN analysis by atomic weight percent.

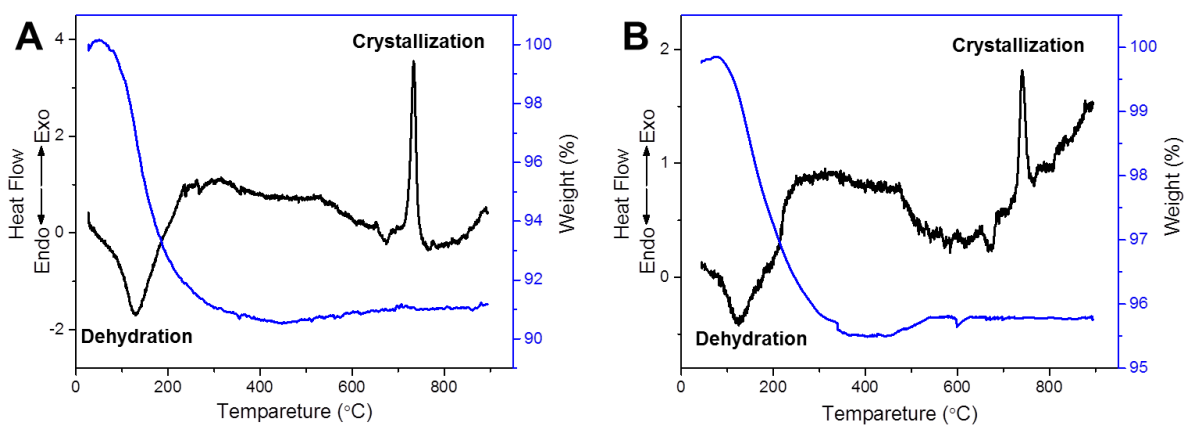


**Figure S8.** Simultaneous DSC-TGA of (A) Ta<sub>2</sub>O<sub>5</sub> nanoplates and (B) Ta<sub>2</sub>O<sub>5</sub> octahedra.

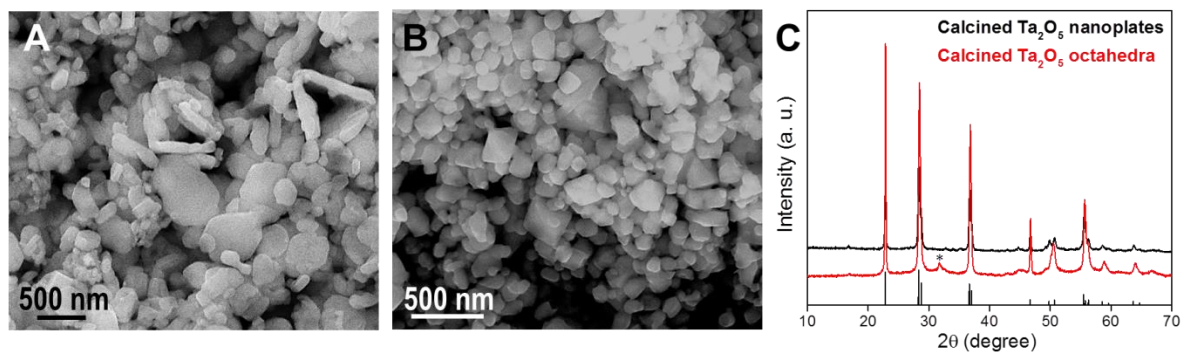


**Figure S9.** SEM images of calcined (A) Ta<sub>2</sub>O<sub>5</sub> nanoplates and (B) Ta<sub>2</sub>O<sub>5</sub> octahedra. (C) The corresponding XRD patterns, with reference Ta<sub>2</sub>O<sub>5</sub> ICDD # 01-089-2843 included. An impurity is denoted with an asterisk.

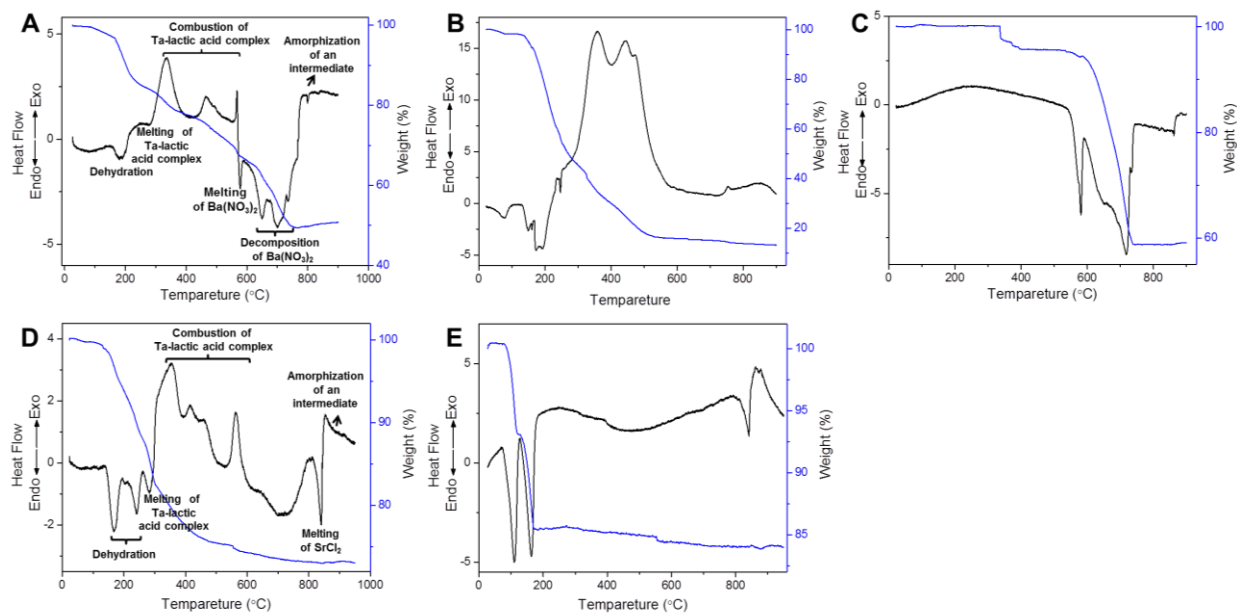


**Figure S10.** TGA (blue curves) and DSC (black curves) of (A) the dried precursor to Ta<sub>2</sub>O<sub>5</sub> nanoplates, (B) the Ta-lactic acid complex, (C) Ba(NO<sub>3</sub>)<sub>2</sub>, (D) the dried precursor to Ta<sub>2</sub>O<sub>5</sub> octahedra, and (E) SrCl<sub>2</sub>.

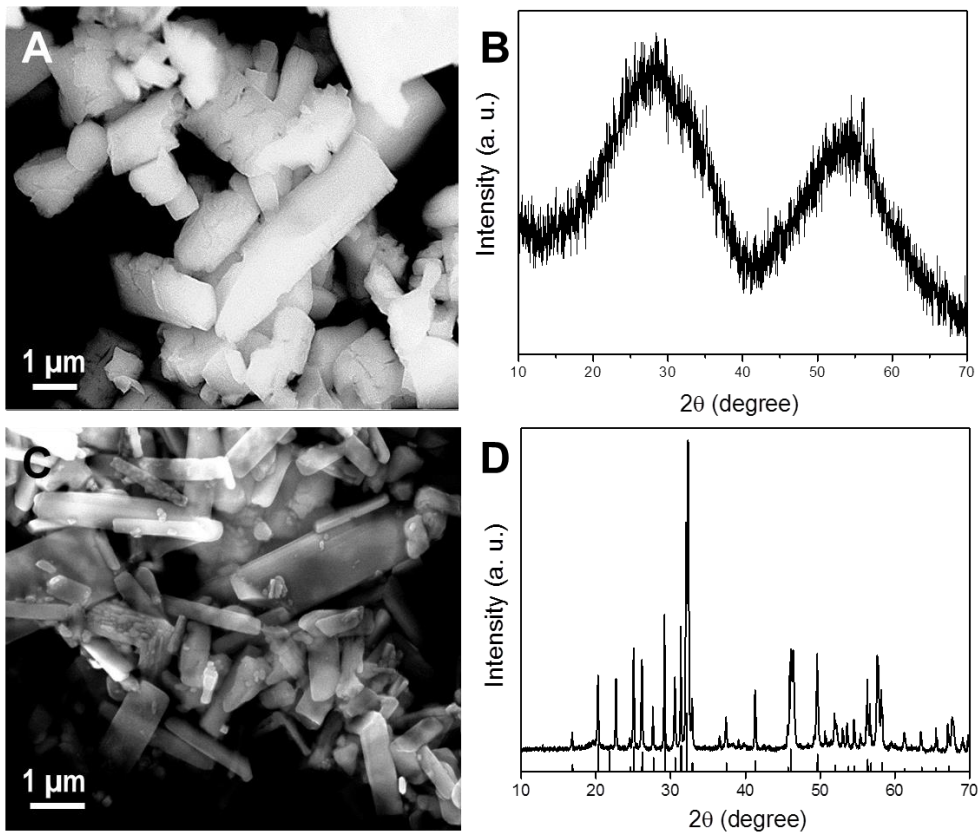


**Figure S11.** (A, C) SEM images and (B, D) XRD patterns of products obtained from heating the dried precursors to (A, B) Ta<sub>2</sub>O<sub>5</sub> nanoplates and (C, D) Ta<sub>2</sub>O<sub>5</sub> octahedra. The Sr<sub>2</sub>Ta<sub>2</sub>O<sub>7</sub> ICDD # 00-030-1304 reference is included in D.

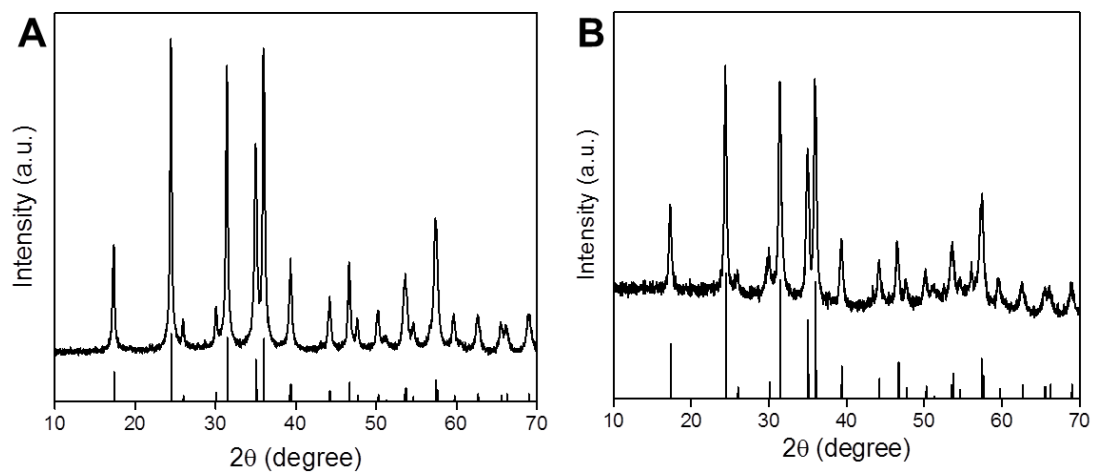


**Figure S12.** XRD patterns of (A) Ta<sub>3</sub>N<sub>5</sub> nanoplates and (B) Ta<sub>3</sub>N<sub>5</sub> octahedra. Ta<sub>3</sub>N<sub>5</sub> ICDD # 01-079-1533 reference included in both.

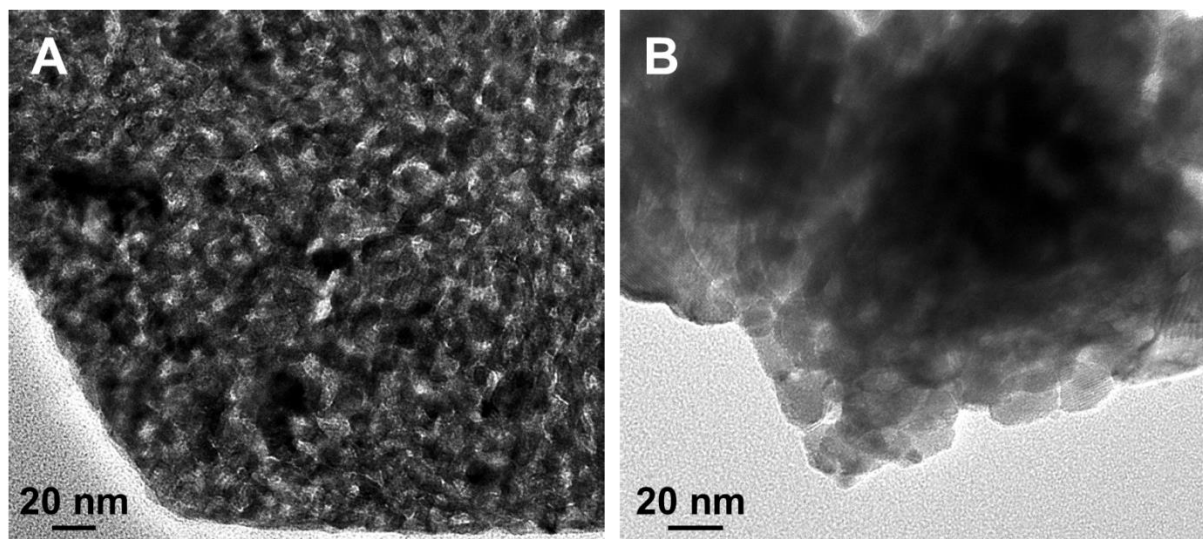


**Figure S13.** Higher magnification TEM images of a (A) Ta<sub>3</sub>N<sub>5</sub> nanoplate and (B) Ta<sub>3</sub>N<sub>5</sub> octahedron.

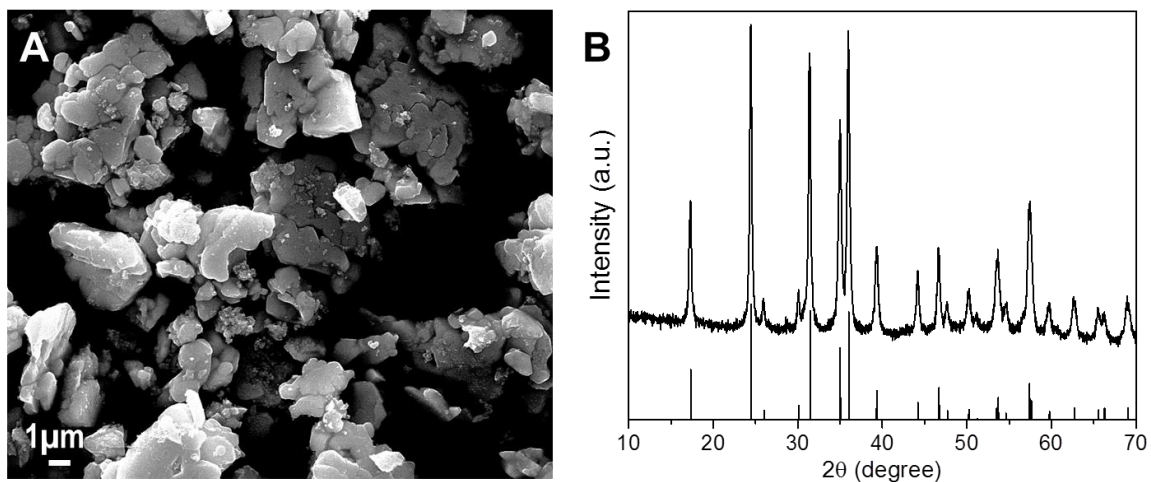


**Figure S14.** (A) SEM image of  $\text{Ta}_3\text{N}_5$  reference from ammonolysis of  $\text{Ta}_2\text{O}_5$  reference and (B) corresponding XRD pattern.  $\text{Ta}_3\text{N}_5$  ICDD # 01-079-1533 reference is included in B.

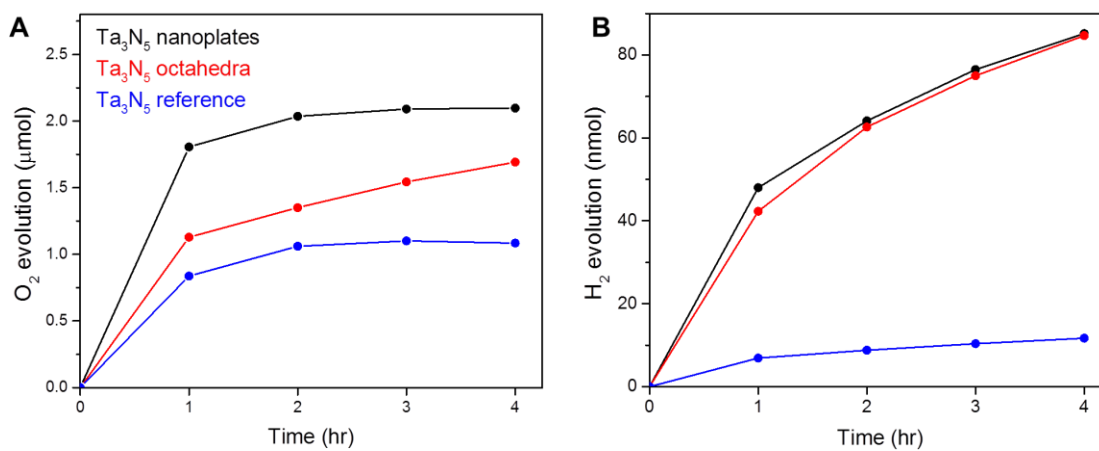


**Figure S15.** (A) OER and (B) HER time study with AMSS-derived nanoplates, octahedra, and reference  $\text{Ta}_3\text{N}_5$  without co-catalyst deposition (photocatalysis conditions: light source: 300 W xenon lamp with a 400 nm long-pass filter. For OER, 20 mg  $\text{Ta}_3\text{N}_5$  and  $\text{La}_2\text{O}_3$  as pH buffer were dispersed in 0.05 M  $\text{AgNO}_3$  solution. For HER, 20 mg  $\text{Ta}_3\text{N}_5$  was dispersed in an aqueous solution containing 10 vol% methanol). The colour notations are the same for both graphs.